

Supplementary: Photoaging of Phenolic Secondary Organic Aerosol in the Aqueous Phase: Evolution of Chemical and Optical Properties and Effects of Oxidants

Wenqing Jiang^{1,2}, Christopher Niedek^{1,2}, Cort Anastasio^{2,3}, Qi Zhang^{1,2*}

5 ¹Department of Environmental Toxicology, University of California, 1 Shields Ave., Davis, CA 95616, USA

²Agricultural and Environmental Chemistry Graduate Program, University of California, 1 Shields Ave., Davis, CA 95616, USA

³Department of Land, Air, and Water Resources, University of California, 1 Shields Ave., Davis, CA 95616, USA

Correspondence to: Qi Zhang (dkwzhang@ucdavis.edu)

Table of Contents

Table of Contents	2
S1. Calculation of the light absorption properties of the aqSOA.....	3
Table S1. The •OH-aqSOA mass yield, H/C, O/C and OS _C determined by HR-ToF-AMS during aqSOA formation and aging.	
15	4
Table S2. The ³ C*-aqSOA mass yield, H/C, O/C and OS _C determined by HR-ToF-AMS during aqSOA formation and aging.	
.....	5
Table S3. Exponential fits for aqSOA formation and decay.....	6
Figure S1. Summary of diagnostic plots of the PMF analysis of the •OH-initiated reactions : (a) Q/Q _{exp} as a function of number	
20 of factors selected for PMF modeling. (b) Q/Q _{exp} as a function of fPeak. (c) Correlations among PMF factors. (d) Box and	
whisker plot showing the distributions of scaled residuals for each AMS ion. (e) Box and whisker plot showing the distributions	
of scaled residuals for each light absorption wavelength. (f) Reconstructed and measured total signal for each sample. (g)	
Q/Q _{exp} for each sample.	7
Figure S2. Summary of diagnostic plots of the PMF analysis of the ³ C*-initiated reactions: (a) Q/Q _{exp} as a function of number	
25 of factors selected for PMF modeling. (b) Q/Q _{exp} as a function of fPeak. (c) Correlations among PMF factors. (d) Box and	
whisker plot showing the distributions of scaled residuals for each AMS ion. (e) Box and whisker plot showing the distributions	
of scaled residuals for each light absorption wavelength. (f) Reconstructed and measured total signal for each sample. (g)	
Q/Q _{exp} for each sample.	8
Figure S3. Evolution of the mass absorption coefficient spectra of the GA •OH-aqSOA.....	9
30 Figure S4. Evolution of the mass absorption coefficient spectra of the GA ³ C*-aqSOA.....	10
Figure S5. Mass absorption coefficient spectra of guaiacyl acetone.	11
Figure S6. AMS spectra of the •OH-aqSOA and ³ C*-aqSOA before and after aging in the dark.....	12
Figure S7. Van Krevelen diagrams that illustrate the evolution trends of the •OH-aqSOA and ³ C*-aqSOA under different	
photoaging conditions.....	13
35 Figure S8. Triangle plots (f _{CO2+} vs f _{C2H3O+}) that depict the evolution trends of the •OH-aqSOA and ³ C*-aqSOA under different	
photoaging conditions.....	14
Figure S9. The plots of f _{CO2+} vs f _{CHO2+} that depict the carboxylic acid formation in the •OH-aqSOA and the ³ C*-aqSOA under	
different photoaging conditions.....	15
Figure S10. Time trend of selected AMS tracer ions in the •OH-aqSOA during aqSOA formation and prolonged aging.	16
40 Figure S11. Time trends of selected AMS tracer ions in the ³ C*-aqSOA during aqSOA formation and prolonged aging.	17

S1. Calculation of the light absorption properties of the aqSOA

The light absorption coefficient ($\alpha_\lambda, \text{cm}^{-1}$) of the aqSOA was calculated as:

$$45 \quad \alpha_\lambda = \frac{A_{\text{total},\lambda} - A_{\text{GA},\lambda} - A_{\text{DMB},\lambda}}{1} \quad (\text{Eq. S1})$$

where $A_{\text{total},\lambda}$ is the total measured base-10 light absorbance of the solution at wavelength λ , $A_{\text{GA},\lambda}$ and $A_{\text{DMB},\lambda}$ denote the absorbance contributed by GA and 3,4-DMB, and 1 is the pathlength of the cuvette (1 cm). The mass absorption coefficient ($\text{MAC}_\lambda, \text{m}^2 \text{ g}^{-1}$) of the aqSOA was calculated as:

$$\text{MAC}_\lambda = \frac{2.303 \times \alpha_\lambda}{[\text{Org}]_{\text{solution}}} \times 100 \quad (\text{Eq. S2})$$

50 where $[\text{Org}]_{\text{solution}}$ is the aqSOA mass concentration ($\mu\text{g mL}^{-1}$) in the solution, 2.303 is a conversion factor between \log_{10} and natural log, and 100 is for unit conversion. The absorption Ångström exponent (AAE) of the aqSOA was calculated as:

$$AAE_{\lambda_1-\lambda_2} = - \frac{\ln \frac{\alpha_{\lambda_1}}{\alpha_{\lambda_2}}}{\ln \frac{\lambda_1}{\lambda_2}} \quad (\text{Eq. S3})$$

where α_{λ_1} and α_{λ_2} denote the light absorption coefficients at wavelengths λ_1 and λ_2 . The rate of sunlight absorption of the aqSOA ($R_{\text{abs}}, \text{mol photons L}^{-1} \text{ s}^{-1}$) was calculated as:

$$55 \quad R_{\text{abs}} = 2.303 \times \frac{10^3}{N_A} \times \sum_{290 \text{ nm}}^{500 \text{ nm}} (\alpha_\lambda \times I_\lambda \times \Delta\lambda) \quad (\text{Eq. S4})$$

where I_λ is the midday winter-solstice actinic flux in Davis (photons $\text{cm}^{-2} \text{ s}^{-1} \text{ nm}^{-1}$) from the Tropospheric Ultraviolet and Visible (TUV) Radiation Model version 5.3 (https://www.acom.ucar.edu/Models/TUV/Interactive_TUV/), $\Delta\lambda$ is the interval between adjacent wavelengths in the TUV output, 2.303 is for base conversion between \log_{10} and natural log, 10^3 is for unit conversion, and N_A is Avogadro's number.

60

Table S1. The •OH-aqSOA mass yield, H/C, O/C and OSc determined by HR-ToF-AMS during aqSOA formation and aging.

	Irradiation Time (h)	SOA yield	H/C	O/C	OSc
•OH-aqSOA formation	0.5	9.72E-01	1.64	0.32	-1.00
	1	8.60E-01	1.52	0.43	-0.66
	2	1.03E+00	1.46	0.51	-0.45
	3	1.06E+00	1.43	0.54	-0.34
	4	9.24E-01	1.43	0.55	-0.33
	6	8.16E-01	1.42	0.57	-0.27
	8	7.39E-01	1.41	0.60	-0.21
	10	6.70E-01	1.41	0.60	-0.21
	12	5.93E-01	1.39	0.62	-0.15
	24	4.60E-01	1.38	0.65	-0.10
•OH-aqSOA aging (no addition of extra oxidant)	25	4.41E-01	1.38	0.66	-0.06
	26	4.31E-01	1.37	0.66	-0.06
	28	4.16E-01	1.37	0.66	-0.06
	30	3.96E-01	1.37	0.67	-0.03
	35	3.55E-01	1.36	0.67	-0.02
	36	3.50E-01	1.36	0.67	-0.02
	40	3.26E-01	1.36	0.67	-0.02
	44	3.05E-01	1.36	0.67	-0.01
	48	2.82E-01	1.36	0.67	-0.02
	60	2.34E-01	1.35	0.67	-0.01
	70	2.07E-01	1.36	0.67	-0.01
	72	2.02E-01	1.35	0.68	0.02
•OH-aqSOA aging (add 100 µM of H2O2)	25	4.54E-01	1.39	0.68	-0.03
	26	4.48E-01	1.39	0.70	0.01
	28	3.74E-01	1.39	0.70	0.01
	30	3.10E-01	1.39	0.70	0.01
	35	1.96E-01	1.40	0.68	-0.04
	36	1.85E-01	1.41	0.66	-0.08
	40	1.56E-01	1.41	0.64	-0.13
	44	1.21E-01	1.40	0.64	-0.12
	48	9.55E-02	1.40	0.64	-0.12
	60	7.43E-02	1.43	0.61	-0.21
	70	6.39E-02	1.44	0.57	-0.29
	72	6.14E-02	1.44	0.57	-0.29
•OH-aqSOA aging (add 5 µM of 3,4-DMB)	25	4.88E-01	1.38	0.66	-0.05
	26	4.48E-01	1.38	0.67	-0.04
	28	4.20E-01	1.37	0.69	0.01
	30	3.99E-01	1.39	0.68	-0.03
	35	2.99E-01	1.40	0.67	-0.05
	36	2.85E-01	1.40	0.67	-0.05
	40	2.40E-01	1.40	0.66	-0.08
	44	2.14E-01	1.41	0.66	-0.09
	48	1.89E-01	1.41	0.65	-0.10
	60	1.37E-01	1.41	0.64	-0.12
	70	1.13E-01	1.42	0.62	-0.17
	72	1.10E-01	1.43	0.61	-0.20
•OH-aqSOA aging (dark)	24	4.29E-01	1.39	0.65	-0.09
	48	4.31E-01	1.39	0.66	-0.07
	72	4.43E-01	1.37	0.66	-0.05

Table S2. The $^{3}\text{C}^*$ -aqSOA mass yield, H/C, O/C and OSC determined by HR-ToF-AMS during aqSOA formation and aging.

	Irradiation Time (h)	SOA yield	H/C	O/C	OSC
$^{3}\text{C}^*$ -aqSOA formation	0.3	/	1.61	0.37	-0.88
	0.6	9.03E-01	1.53	0.43	-0.67
	0.9	8.90E-01	1.50	0.46	-0.58
	1.2	8.83E-01	1.49	0.48	-0.52
	1.7	8.69E-01	1.48	0.51	-0.46
	2.3	8.58E-01	1.47	0.54	-0.39
	2.9	8.50E-01	1.46	0.54	-0.38
	3.5	8.58E-01	1.44	0.58	-0.29
	3.8	8.39E-01	1.43	0.60	-0.23
	4.1	8.52E-01	1.43	0.62	-0.17
$^{3}\text{C}^*$ -aqSOA aging (no addition of extra oxidant)	4.3	8.45E-01	1.42	0.64	-0.15
	4.6	8.23E-01	1.43	0.65	-0.13
	4.9	8.13E-01	1.43	0.64	-0.15
	5.2	8.02E-01	1.42	0.68	-0.06
	5.8	7.80E-01	1.42	0.71	-0.01
	6.4	7.49E-01	1.42	0.73	0.03
	7.0	7.16E-01	1.42	0.74	0.05
	8.1	6.33E-01	1.43	0.75	0.06
	9.3	5.76E-01	1.43	0.76	0.10
	11.6	5.05E-01	1.43	0.77	0.11
	13.9	4.43E-01	1.43	0.77	0.12
	3.8	8.44E-01	1.44	0.59	-0.24
	4.1	8.42E-01	1.43	0.62	-0.17
	4.3	8.33E-01	1.42	0.65	-0.12
$^{3}\text{C}^*$ -aqSOA aging (add 100 μM of H_2O_2)	4.6	8.04E-01	1.43	0.68	-0.06
	4.9	7.95E-01	1.42	0.70	-0.02
	5.2	7.83E-01	1.42	0.70	-0.01
	5.8	7.52E-01	1.41	0.72	0.03
	6.4	7.14E-01	1.41	0.73	0.05
	7.0	6.85E-01	1.42	0.74	0.07
	8.1	6.30E-01	1.42	0.75	0.08
	9.3	5.70E-01	1.43	0.76	0.10
	11.6	4.89E-01	1.45	0.74	0.02
	13.9	3.81E-01	1.45	0.76	0.07
	3.8	8.48E-01	1.42	0.58	-0.30
	4.1	8.44E-01	1.42	0.59	-0.28
	4.3	8.50E-01	1.42	0.59	-0.26
$^{3}\text{C}^*$ -aqSOA aging (add 5 μM of 3,4-DMB)	4.6	8.46E-01	1.42	0.59	-0.22
	4.9	8.41E-01	1.43	0.61	-0.19
	5.2	8.41E-01	1.43	0.61	-0.18
	5.8	8.31E-01	1.41	0.63	-0.15
	6.4	8.22E-01	1.42	0.65	-0.12
	7.0	8.08E-01	1.42	0.66	-0.09
	8.1	7.73E-01	1.42	0.68	-0.07
	9.3	7.45E-01	1.42	0.69	-0.04
	11.6	6.82E-01	1.43	0.70	-0.02
	13.9	6.38E-01	1.43	0.71	-0.02
$^{3}\text{C}^*$ -aqSOA aging (dark)	7.0	9.05E-01	1.44	0.59	-0.26
	13.9	9.25E-01	1.43	0.60	-0.24

Table S3. Exponential fits for aqSOA formation and decay

	Pseudo-first-order decay of GA	Exponential fit for initial aqSOA formation	Exponential fit for aqSOA decay
•OH-aqSOA	$[GA]_t/[GA]_0 = e^{-0.144t}$	$y = 14.8(1 - e^{-0.167x})$	No addition of extra oxidant: $y = 7.4e^{-0.017x}$
			Add 100 μM of H ₂ O ₂ : $y = 6.6e^{-0.11x} + 1.08$
			Add 5 μM of 3,4-DMB: $y = 6.3e^{-0.057x} + 1.44$
³ C*-aqSOA	$[GA]_t/[GA]_0 = e^{-0.727t}$	$y = 14.5(1 - e^{-0.945x})$	No addition of extra oxidant: $y = 15.1e^{-0.073x}$
			Add 100 μM of H ₂ O ₂ : $y = 15.3e^{-0.078x}$
			Add 5 μM of 3,4-DMB: $y = 15.7e^{-0.034x}$

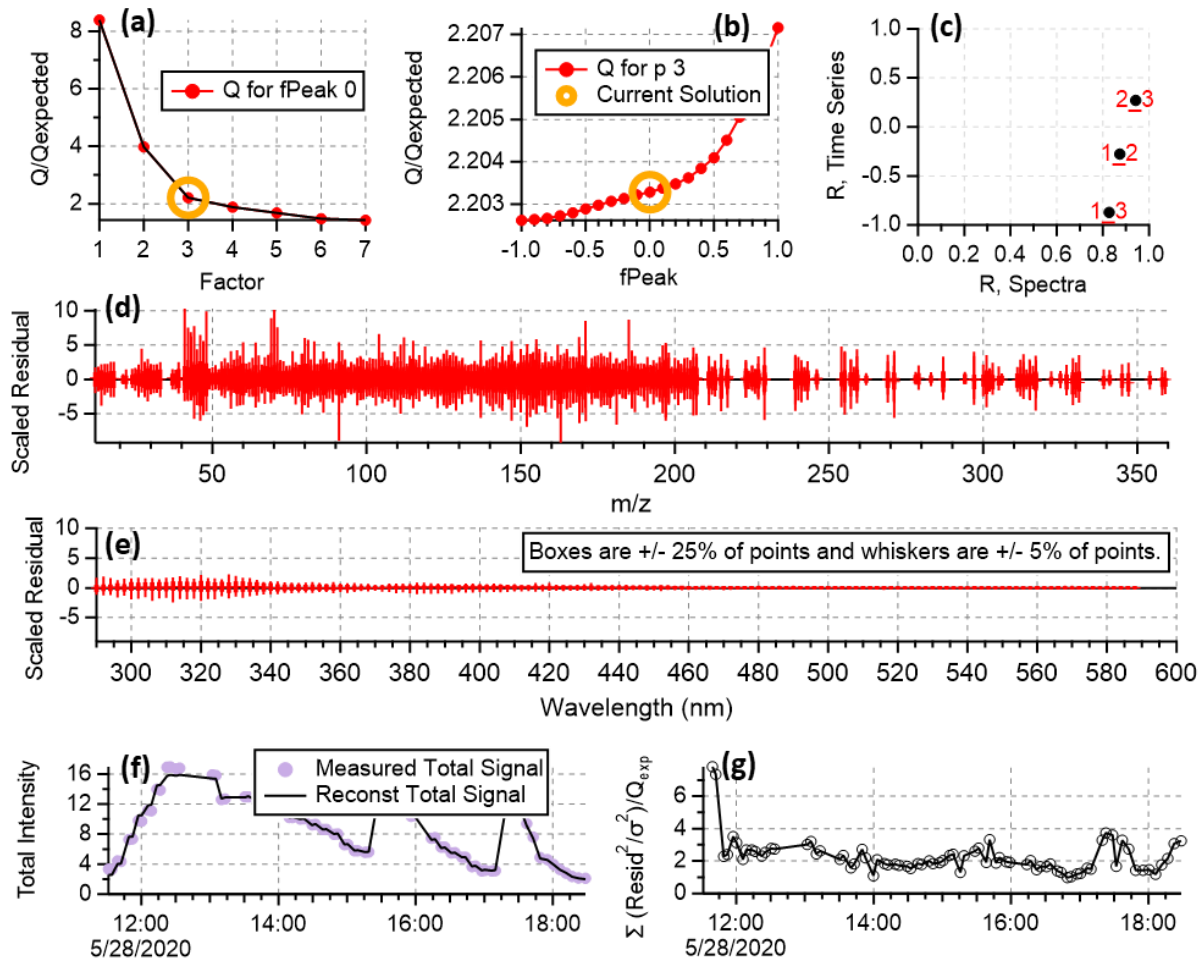
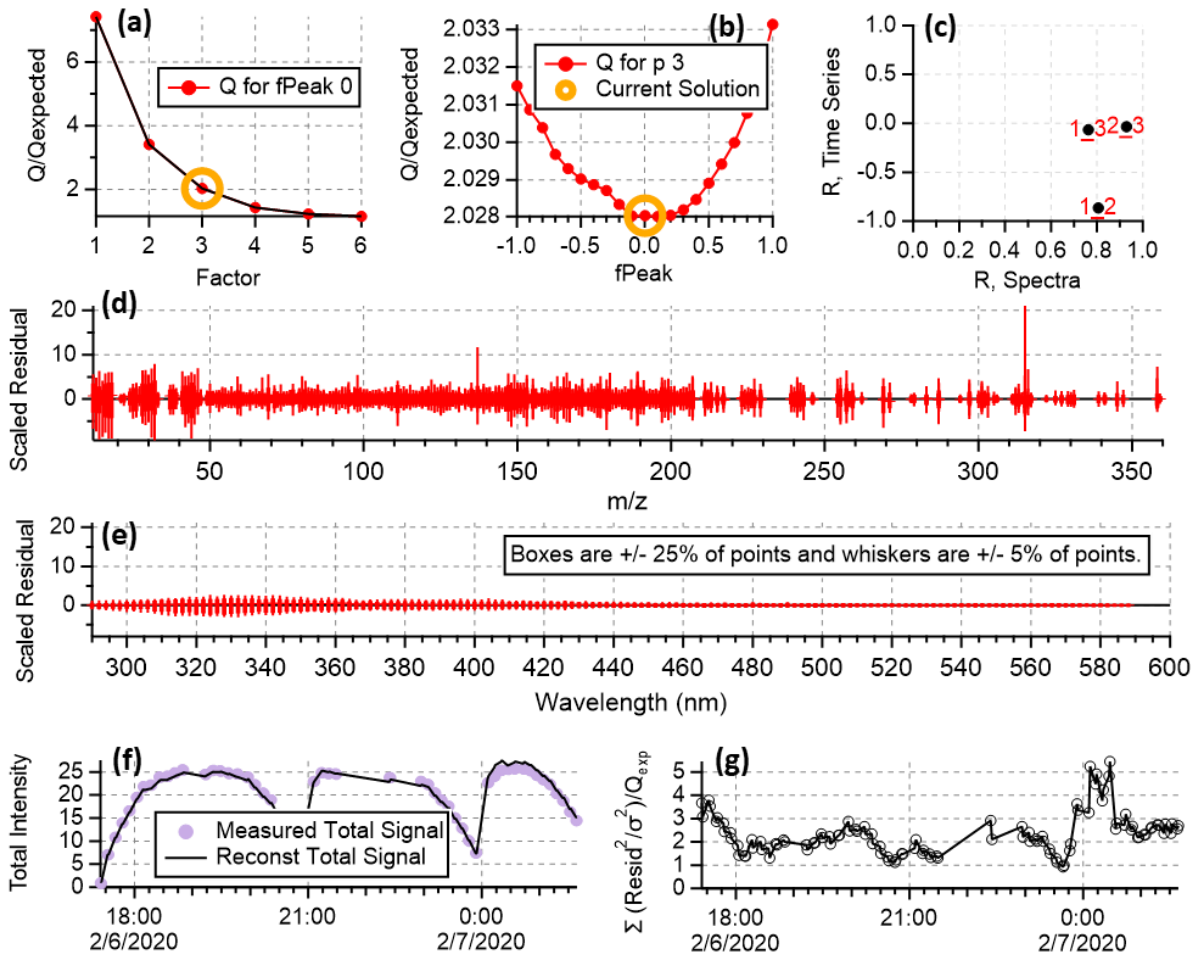
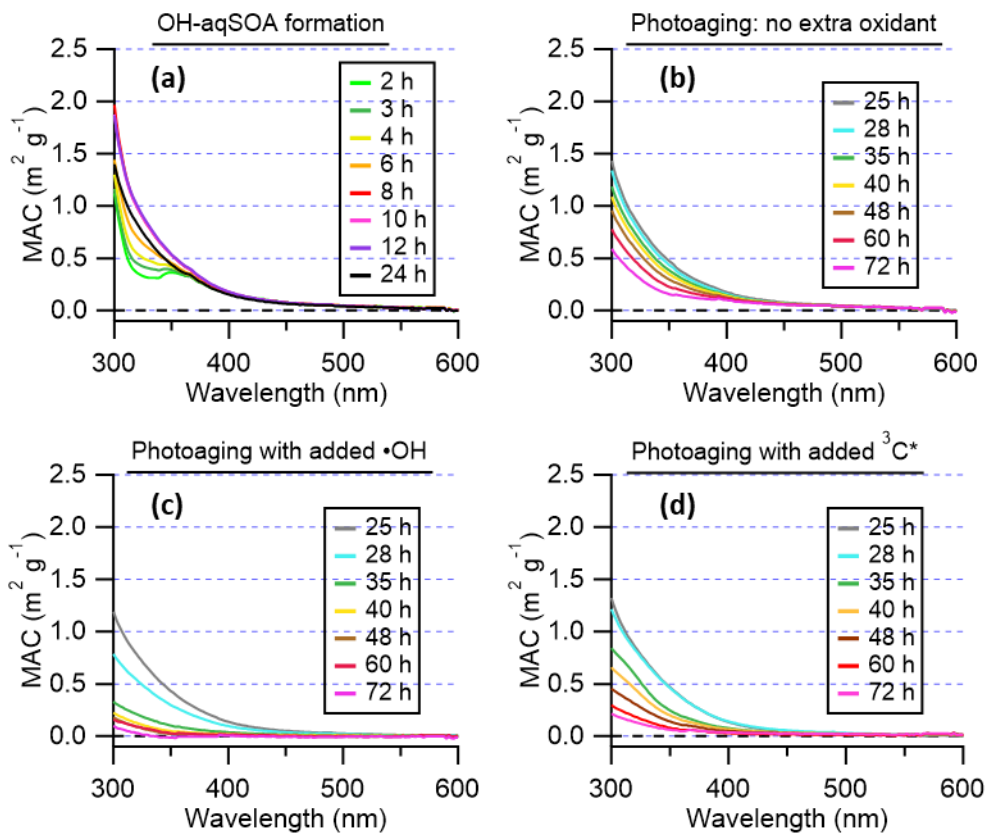


Figure S1. Summary of diagnostic plots of the PMF analysis of the $\bullet\text{OH}$ -initiated reactions : (a) Q/Q_{exp} as a function of number of factors selected for PMF modeling. (b) Q/Q_{exp} as a function of fPeak. (c) Correlations among PMF factors. (d) Box and whisker plot showing the distributions of scaled residuals for each AMS ion. (e) Box and whisker plot showing the distributions of scaled residuals for each light absorption wavelength. (f) Reconstructed and measured total signal for each sample. (g) Q/Q_{exp} for each sample.



75

Figure S2. Summary of diagnostic plots of the PMF analysis of the ${}^3\text{C}^*$ -initiated reactions: (a) Q/Q_{exp} as a function of number of factors selected for PMF modeling. (b) Q/Q_{exp} as a function of fPeak. (c) Correlations among PMF factors. (d) Box and whisker plot showing the distributions of scaled residuals for each AMS ion. (e) Box and whisker plot showing the distributions of scaled residuals for each light absorption wavelength. (f) Reconstructed and measured total signal for each sample. (g) Q/Q_{exp} for each sample.



80

Figure S3. Evolution of the mass absorption coefficient spectra of the GA $\cdot\text{OH}$ -aqSOA.

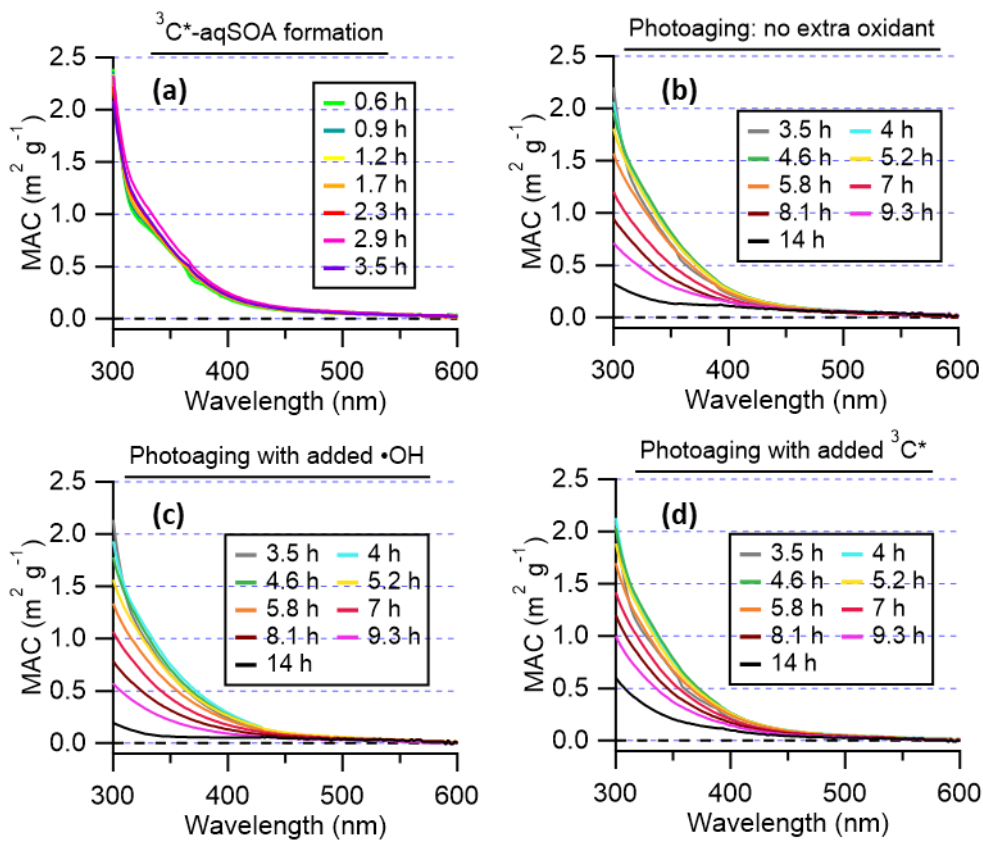


Figure S4. Evolution of the mass absorption coefficient spectra of the GA ${}^3\text{C}^*$ -aqSOA.

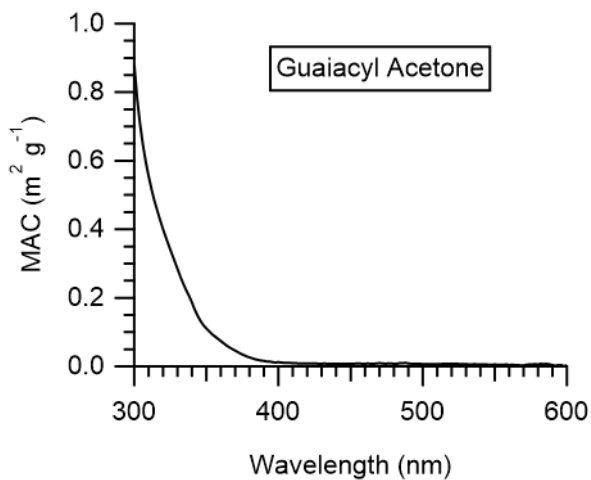
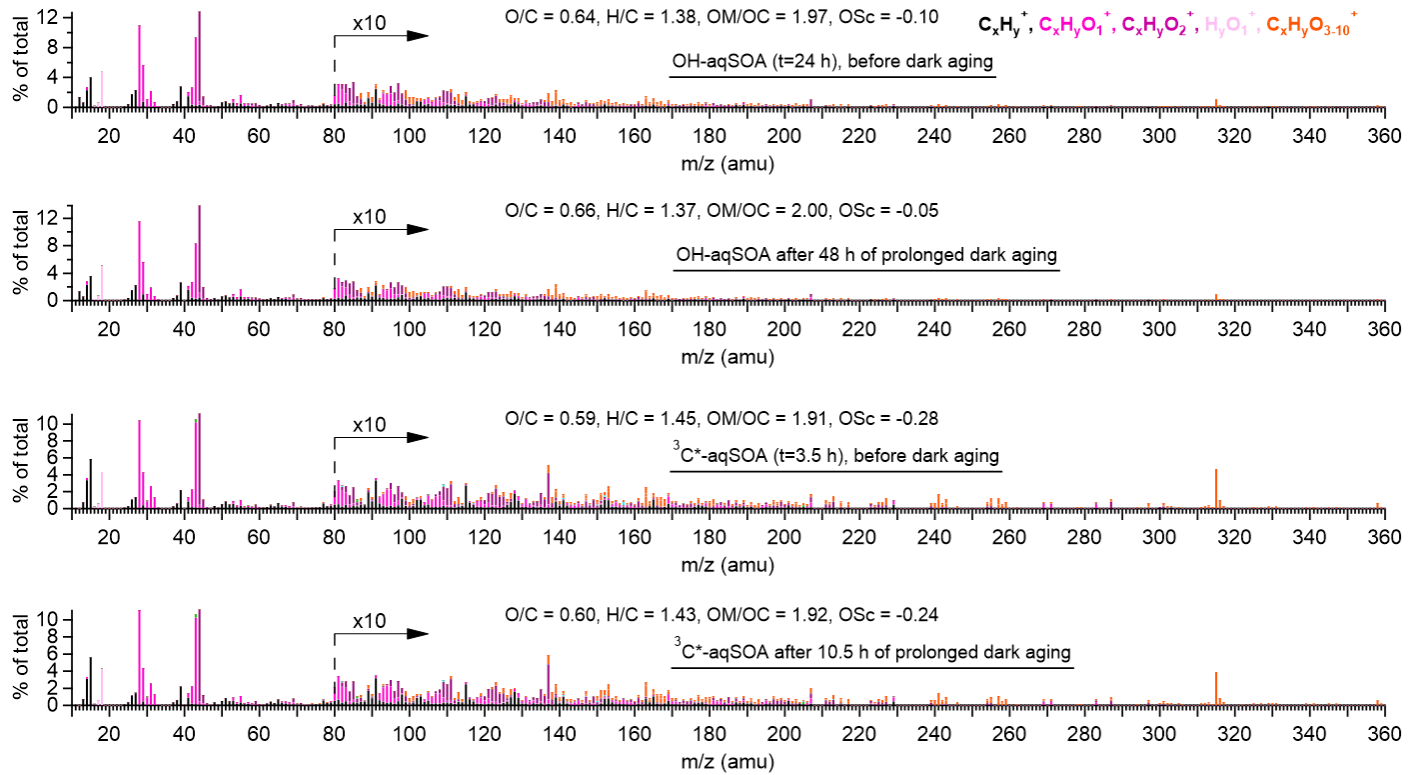


Figure S5. Mass absorption coefficient spectra of guaiacyl acetone.



90 Figure S6. AMS spectra of the •OH-aqSOA and $^{3}\text{C}^*$ -aqSOA before and after aging in the dark

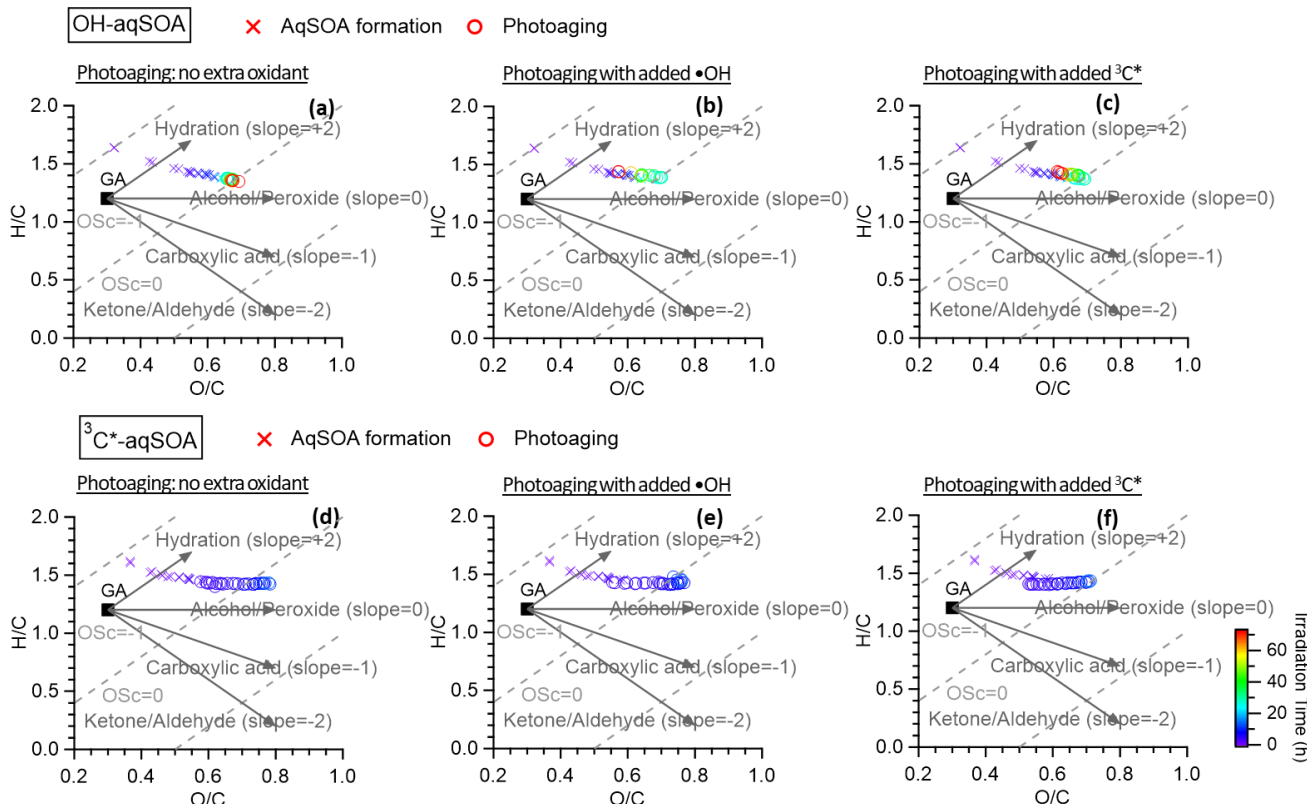


Figure S7. Van Krevelen diagrams that illustrate the evolution trends of the •OH-aqSOA and ³C*-aqSOA under different photoaging conditions.

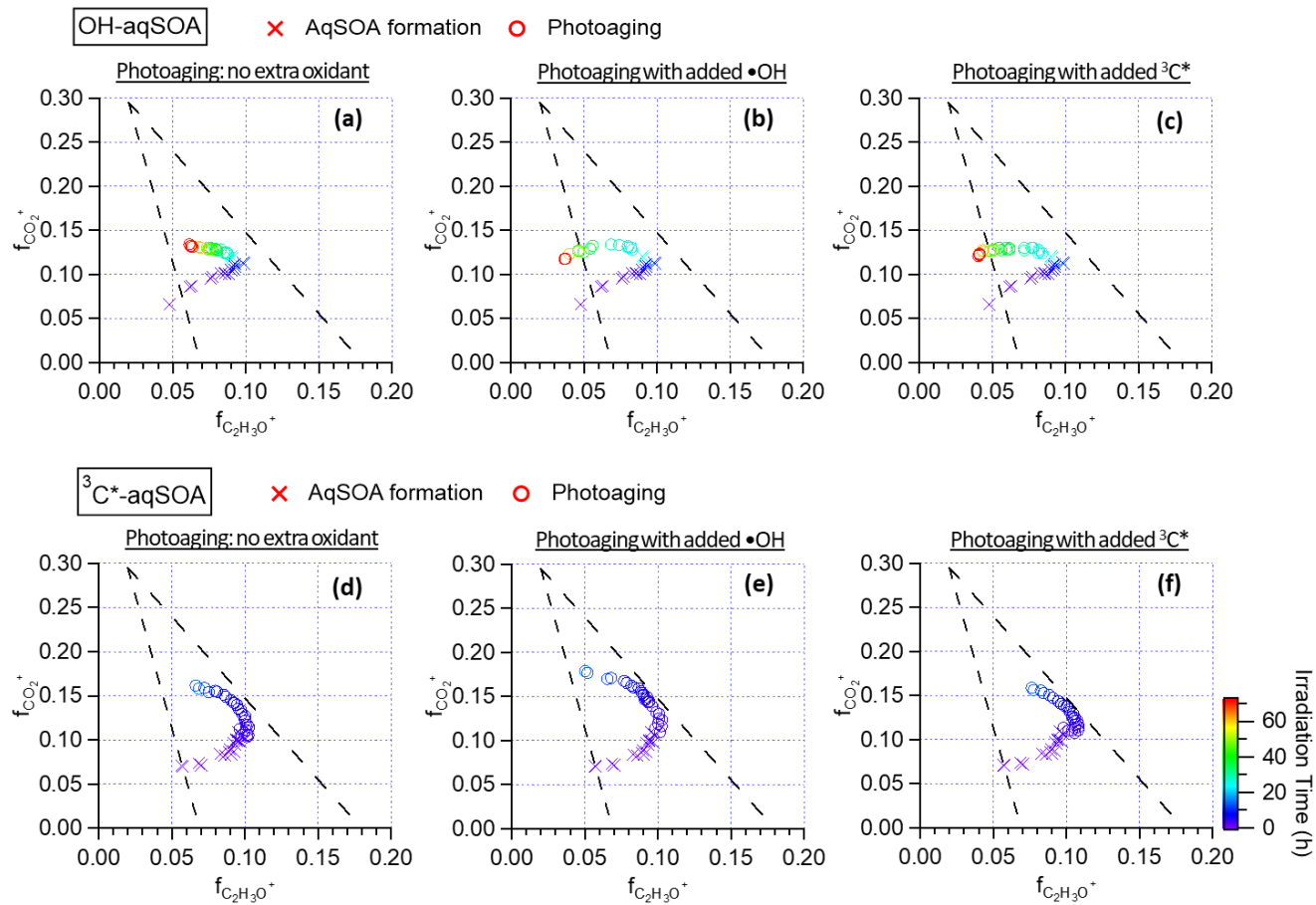


Figure S8. Triangle plots ($f_{CO_2^+}$ vs $f_{C_2H_3O^+}$) that depict the evolution trends of the $\bullet OH$ -aqSOA and $^3C^*$ -aqSOA under different photoaging conditions.

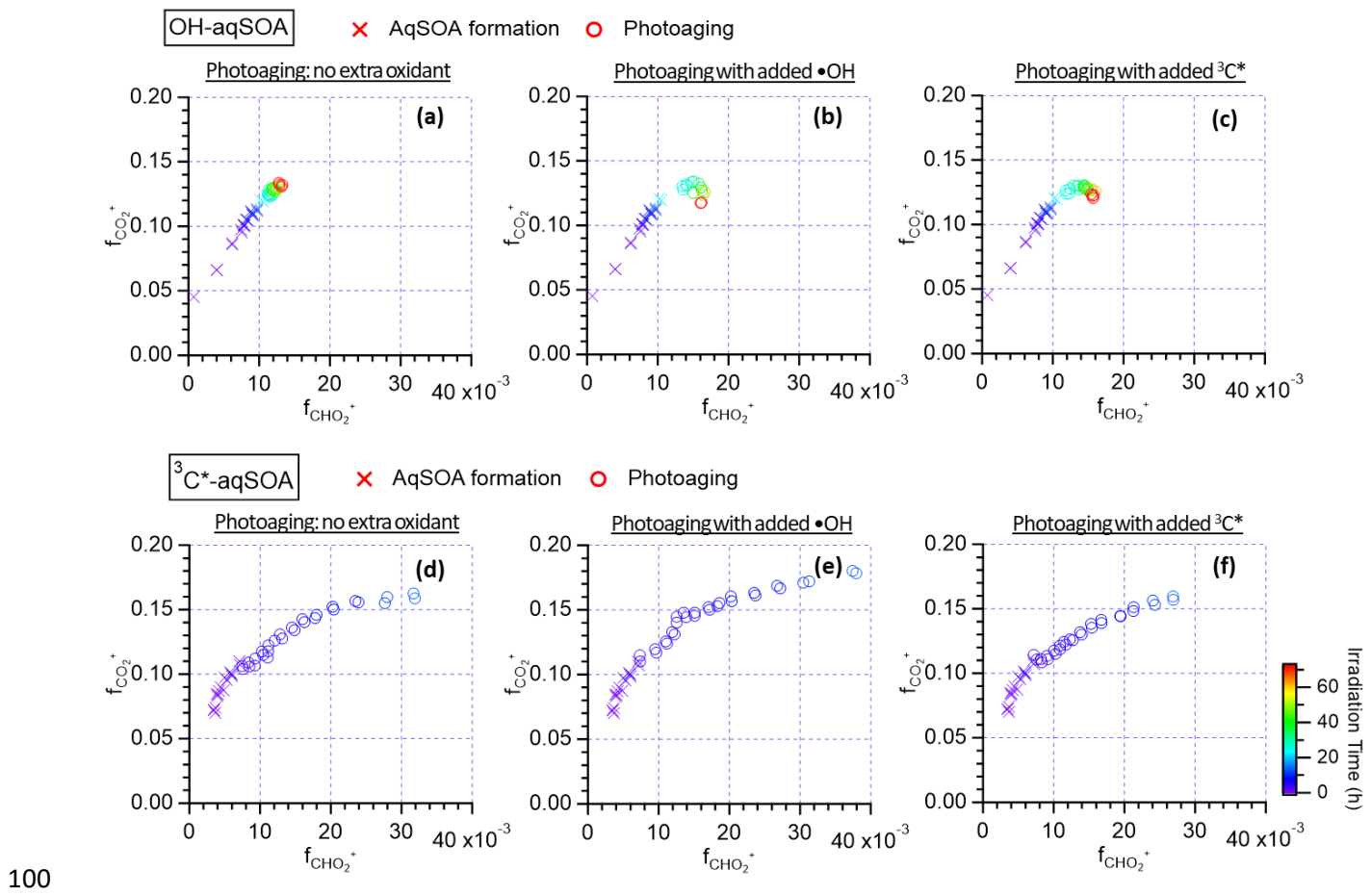
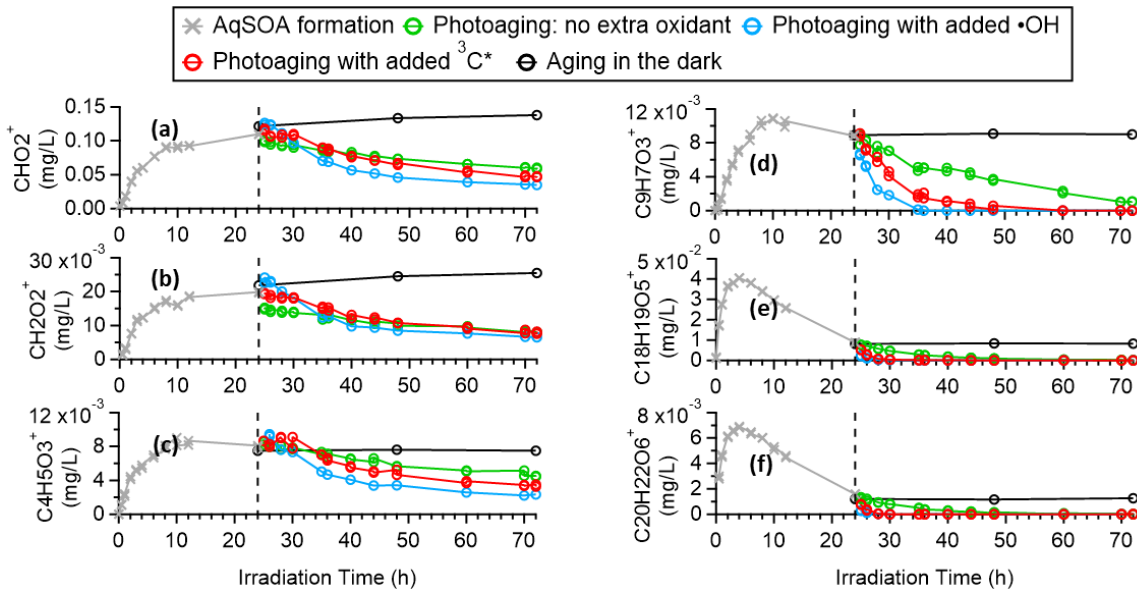


Figure S9. The plots of $f_{\text{CO}_2^+}$ vs $f_{\text{CHO}_2^+}$ that depict the carboxylic acid formation in the $\bullet\text{OH}$ -aqSOA and the $^3\text{C}^*$ -aqSOA under different photoaging conditions.



105 Figure S10. Time trend of selected AMS tracer ions in the •OH-aqSOA during aqSOA formation and prolonged aging.

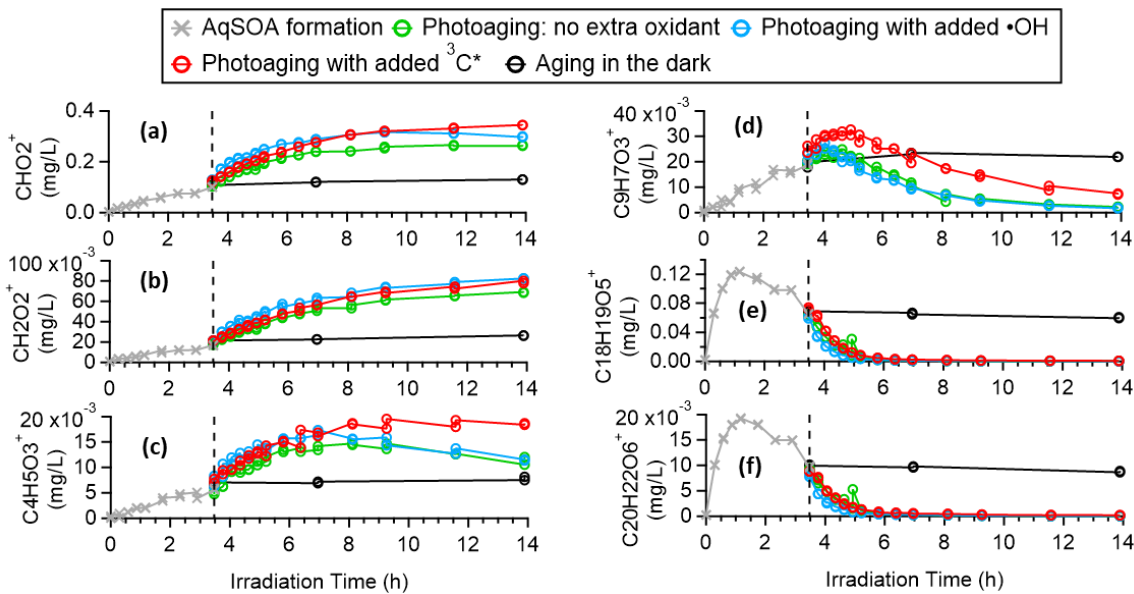


Figure S11. Time trends of selected AMS tracer ions in the $^{3}\text{C}^*$ -aqSOA during aqSOA formation and prolonged aging.